Long-Term Stability at High Temperatures for Birefringence in PAZO/PAH Layer-by-Layer Films

ARTICLE *in* ACS APPLIED MATERIALS & INTERFACES · MARCH 2012

Impact Factor: 6.72 · DOI: 10.1021/am201722x · Source: PubMed

4 AUTHORS:

Quirina Ferreira
Institute of Telecommunications
38 PUBLICATIONS **239** CITATIONS
SEE PROFILE

Paulo Ribeiro
New University of Lisbon
51 PUBLICATIONS **481** CITATIONS
SEE PROFILE

Osvaldo N Oliveira
University of São Paulo
531 PUBLICATIONS **8,962** CITATIONS
SEE PROFILE

Maria Raposo
New University of Lisbon
60 PUBLICATIONS **842** CITATIONS
SEE PROFILE

ACS APPLIED MATERIALS & INTERFACES

Research Article

www.acsami.org

Long-Term Stability at High Temperatures for Birefringence in PAZO/PAH Layer-by-Layer Films

Quirina Ferreira,[†,‡] Paulo A. Ribeiro,[†] Osvaldo N. Oliveira, Jr.,[§] and Maria Raposo*[,†]

[†]CEFITEC, Departamento de Física, Faculdade de Ciências e Tecnologia, Universidade Nova de Lisboa (FCT/UNL), 2829-516 Caparica, Portugal

[‡]Instituto de Telecomunicações, Instituto Superior Técnico, Av. Rovisco Pais, P-1049-001 Lisboa, Portugal

[§]Instituto de Física de São Carlos, Universidade de São Paulo, CP 369, 13560-970, São Carlos, São Paulo, Brazil

Supporting Information

ABSTRACT: Optical memories with long-term stability at high temperatures have long been pursued in azopolymers with photoinduced birefringence. In this study, we show that the residual birefringence in layer-by-layer (LbL) films made with poly[1-[4-(3-carboxy-4 hydroxyphenylazo)benzene sulfonamido]-1,2-ethanediyl, sodium salt] (PAZO) alternated with poly(allylamine hydrochloride) (PAH) can be tuned by varying the extent of electrostatic interactions with film fabrication at different pHs for PAH. The dynamics of both writing and relaxation processes could be explained with a two-stage mechanism involving the orientation of the chromophores per se and the chain movement. Upon calculating the activation energies for these processes, we demonstrate semiquantitatively that reduced electrostatic interactions in films prepared at higher pH, for which PAH is less charged, are responsible for the longer stability at high temperatures. This is attributed to orientation of PAZO chromophores via cooperative aggregation, where the presence of counterions hindered relaxation.

KEYWORDS: *azo-chromophore, layer-by-layer, counterions, cooperative aggregation, long-term stability, birefringence, PAZO*

INTRODUCTION

The use of photorefractive materials in organic photonics applications, such as optical memories and surface-relief gratings with antireflecting properties, requires long-term stability of the light-induced changes in the refractive index, even at high temperatures. The main thrust in the search for novel materials with enhanced optical properties for those applications has focused on the molecular control that can be achieved with some fabrication techniques. For nanostructured polymer films, for instance, various methods have been used, including the layer-by-layer (LbL) technique based on the adsorption of oppositely charged materials.[1−4] With the LbL method, one is able to produce supramolecular architectures, where not only the thickness and composition can be controlled precisely, but also their properties may be tuned synergistically with a combination of distinct materials in the same film. Examples of synergistic activity may be found in various areas, such as in sensors and biosensors[5] or organic light-emitting diodes.[6−9] LbL films made with azopolymers,[10−17] in particular, may have their photoinduced properties altered by varying the electrostatic interactions responsible for the film formation.[18] The interest in azopolymers arises mainly from the photoisomerization of the azochromophore from *trans* to *cis* isomers that leads to birefringence.[19−24] This photoisomerization is achieved by impinging light of adequate wavelength on the film, which induces a change in molecular conformation and molecular reorientation after several *trans*−*cis*−*trans* photoisomerization cycles. The azochromophores will tend to align perpendicular to the polarization direction of the electric field of the incoming light.

One challenge in using azopolymers in optical memories is to guarantee long-term stability for the photoinduced birefringence, and at high temperatures. The physical properties of polymers depend significantly on temperature, especially near the glass-transition temperature (T_g), where polymer chains have their mobility increased. Birefringence is relatively stable below the azopolymer T_g[25] value and is erasable by heating the polymer to this temperature. Therefore, in order to obtain long-term storage optical devices, one must seek polymers with good thermal stability and high T_g values. Several reports have been made in the literature with this purpose. These include photoactive polymers with high T_g values,[26−30] ionic complexes,[31] and LbL films based on a high T_g azopolyelectrolyte that displayed stable induced dichroism.[32] Other strategies to prepare stable birefringent materials should nevertheless be considered, and the possible tuning of photoisomerization and reorientation processes with changes on the electrostatic interactions in LbL films has motivated us to institute research into the dynamics of birefringence creation and relaxation at distinct temperatures.

In this study, we used films containing poly[1-[4-(3-carboxy-4 hydroxyphenylazo)benzene sulfonamido]-1,2-ethanediyl, sodium salt] (PAZO), which is an azopolymer with ionized groups, alternated with the polyelectrolyte poly(allylamine hydrochloride) (PAH), where the latter layers were adsorbed at different pHs (i.e., with different degrees of ionization) in order to tune the electrostatic interactions. A semiquantitative

Received: December 6, 2011
Accepted: February 15, 2012
Published: February 15, 2012

   dx.doi.org/10.1021/am201722x | ACS Appl. Mater. Interfaces 2012, 4, 1470−1477

treatment for the kinetics of writing and relaxation of the photoinduced birefringence will be provided, which may be useful to guide the search for stable optical devices at high temperatures.

MATERIALS AND METHODS

The LbL films were prepared from poly[1-[4-(3-carboxy-4 hydroxyphenylazo)benzene sulfonamido]-1,2-ethanediyl, sodium salt] (PAZO) and poly(allylamine hydrochloride) (PAH) (average M_w = 50 000−65 000 g/mol), obtained from Aldrich, whose chemical structures are shown in Figure 1.

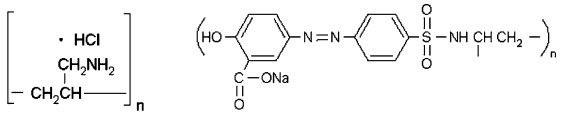

Figure 1. Chemical structures of (a) poly(allylamine hydrochloride) (PAH) and (b) poly[1-[4-(3-carboxy-4 hydroxyphenylazo)benzene sulfonamido]-1,2-ethanediyl, sodium salt] (PAZO).

PAZO was dissolved in pure water supplied by a Milli-Q system from Millipore (resistivity = 18 MΩ cm) to a concentration of 10^{-2} M with pH ca. 9. The PAH aqueous solutions had a concentration of 10^{-2} M and a pH that was varied by adding either HCl or NaOH. The PAZO/PAH LbL films were adsorbed onto glass substrates that had been hydrophilized in a Piranha solution for 30 min. Deposition comprised the following steps: (i) immersion of the substrate in PAH solution for 30 s; (ii) washing the substrate + PAH layer with pure water; (iii) immersion of the substrate + PAH layer into the PAZO solution for 30 s; (iv) washing the substrate + PAH/PAZO bilayer with pure water. By repeating steps (i) through (iv), a large number of bilayers could be deposited.

The experimental setup for optical storage measurements is similar to that described in refs 33−38. The 488- and 514-nm lines of a tunable Ar^+ laser were used as writing beams for inducing birefringence. The photoinduced birefringence was measured with a low power, ca. 1 mW, 633-nm HeNe laser beam, referred to as the probe beam, with the sample placed between crossed polarizers. The induced birefringence (Δn) was calculated from the measured light intensity passing through the crossed polarizers, using[38]

$$\Delta n = \frac{\lambda}{\pi l} \sin^{-1} \sqrt{\frac{I}{I_0}} \qquad (1)$$

where λ is the wavelength of the probe beam, l the film thickness, I_0 the incident beam intensity, and I the intensity after the analyzer.

Differential scanning calorimetry (DSC) analysis was performed with a Shimadzu Model Twi50 system, with the PAZO and PAH polyelectrolytes samples heated from ambient temperature up to 225 °C at a heating rate of 10 °C/min and under an inert atmosphere of nitrogen. The thermogravimetric analysis (TGA) was made in a calorimeter model TA 2910, where the thermograms were measured at a heating rate of 10 °C/min under 20 mL/min of synthetic air flow. The LbL films were characterized using Fourier transform infrared (FTIR) spectroscopy with a Mattson spectrophotometer and ultraviolet−visible light (UV-Vis) spectroscopy with a Shimadzu UV-2101PC spectrophotometer.

RESULTS AND DISCUSSION

Photoinduced birefringence in azobenzene-containing films is known[37] to be generated by the movement of chromophores responding to the repeated *trans*−*cis*−*trans* photoisomerization cycles. After a given cycle, the chromophores can be oriented in any direction, and those with their dipole moment perpendicular to the direction of the writing laser polarization will no longer undergo photoisomerization. Therefore, after a series of cycles, there will be a larger number of chromophores perpendicular to the polarization direction than in any other direction, thus leading to the birefringence. This process obviously is dependent on the free volume available for the chromophores to isomerize and reorient, which, in turn, is dependent on the temperature and molecular interactions with the medium. The effects from the temperature on photoisomerization processes in azopolymers have been investigated in cast and spin-coating films,[36−40] and in LbL films.[41] For the latter, the other relevant factor was the degree of ionization.[42] Here, we produced PAZO/PAH LbL films with PAH solutions at pH 4, 6 and 8, whose degrees of ionization were 0.95, 0.9 and 0.7, respectively, according to Choi and Rubner.[43] While adsorbing the PAZO layers, a pH 9 solution was used, at which its degree of ionization is 0.8.[42] Because the pH affects the electrical charge density of weak polyelectrolytes such as PAH,[44] swelling/deswelling of LbL films made with weak polyelectrolytes occur when they are treated or stored at different pHs. Treatment in water at neutral pH for long times affects the degree of ionization of PAH free amine groups due to elimination/reestablishment of hydrophobically associated PAH chain segments, thus leading to molecular rearrangement.[44,45] In the LbL films studied here, both PAH and PAZO are weak polyelectrolytes; therefore, the polymer chains may be organized in different ways, depending on the pH used for adsorption, even before the experiments of photoinduced birefringence.

Because we wished to investigate temperature effects on the photoinduced properties of PAH/PAZO LbL films, we had to ensure that thermal treatments up to 100 °C did not affect the chemical structure of the polymers. In subsidiary experiments, we characterized the polymers with DSC to obtain their T_g values, which were 95 ± 5 °C for PAZO and 91 ± 5 °C for PAH (see the Supporting Information). From thermogravimetry, we observed that, up to 100 °C, there is only some small mass loss, because of the release of water. Moreover, upon heating, no chemical changes were noted with FTIR spectroscopy (see the Supporting Information).

Dynamics of Birefringence Buildup and Relaxation. The 20-bilayer PAH/PAZO LbL films $(PAH/PAZO)_{20}$ were heated to various temperatures, from room temperature (25 °C) up to 100 °C, through the PAZO and PAH glass-transition temperature regions. The residual birefringence was erased with circularly polarized light before each experiment in which the birefringence buildup was studied. The writing and relaxation curves were obtained as a function of time for each temperature, as shown in Figure 2a for $(PAH/PAZO)_{20}$ LbL films prepared from PAZO aqueous solutions at pH 9 and PAH aqueous solutions at pH 4. Similar curves were obtained for films with PAH solutions at pH 6 and pH 8, and, therefore, they have been omitted here. The maximum in birefringence decreased with increasing temperatures. Moreover, for the samples prepared at pH(PAH) 8, there was no significant relaxation (when there was no writing beam) for temperatures

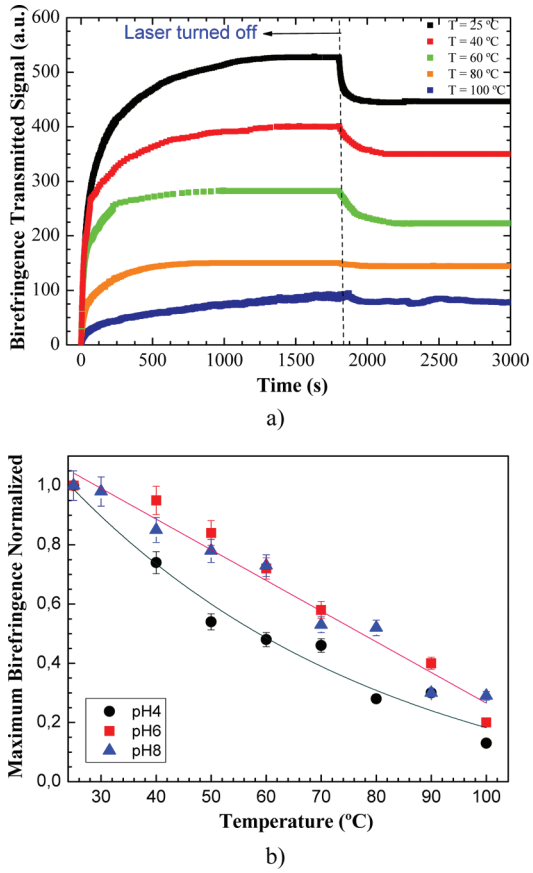

Figure 2. (a) Birefringence buildup and relaxation kinetics curves at different temperatures for $(PAH/PAZO)_{20}$ films prepared from PAH aqueous solutions at pH(PAH) 4. (b) Maximum intensity of normalized birefringence for $(PAH/PAZO)_{20}$ LbL films prepared from PAH solutions with different pHs. The solid lines are only in place to guide the eyes.

of 80 °C or higher. The buildup of birefringence was normalized for all samples taking, as unity, the value at 25 °C. Figure 2b shows the maximum intensity of normalized birefringence curves for $(PAH/PAZO)_{20}$ LbL films prepared from PAH solutions with different pHs. With increasing temperature, the relative percentage of oriented chromophores decreased quasi-linearly, and the decrease varied with pH. For pH(PAH) 4, the intensity of the birefringence normalized signal decreased more significantly, attaining 0.1 at 100 °C (10% of the value at room temperature), than for pH(PAH) 6 and pH(PAH) 8 for which the induced birefringence had practically the same behavior. At 100 °C the normalized birefringence reached 0.2 and 0.3 for samples prepared at pH(PAH) 6 and pH(PAH) 8, respectively.

Since the films were prepared from PAH solutions at different pHs, the adsorbed amounts of PAH and PAZO could differ. The adsorbed amount per unit area (Γ) of PAZO was estimated using the UV−Vis spectra data of the LbL films shown in Figure 3, assuming the absorption coefficient at 360 nm, where only PAZO absorbs, to be 4.30 ± 0.07 g^{-1} m^2.[46] This adsorbed amount of PAZO increased with the pH of the PAH aqueous solutions, which is consistent with the increased birefringence at higher pHs, because the birefringence is expected to be proportional to the number of PAZO chromophores. As shown in the inset of Figure 3, the birefringence normalized by the amount of adsorbed PAZO

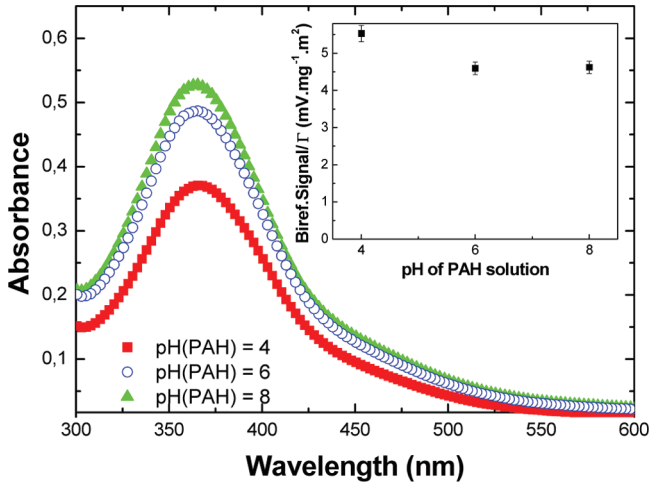

Figure 3. Visible absorption spectra of $(PAH/PAZO)_{20}$ LbL films prepared from different pHs. The inset shows the birefringence signal per adsorbed amount, as a function of the pH of the PAH aqueous solutions.

is practically the same for pH 6 and pH 8, being ca. 20% higher at pH 4. For the latter, the higher birefringence could be explained either by a facilitated orientation of the chromophores or by enhancement due to aggregation.[16,47] The first hypothesis is unlikely because, at pH 4, the stronger electrostatic interactions tend to preclude reorientation, as will be shown in the discussion of the writing kinetics.

The hypothesis of dye aggregation may be examined by considering the shape and position of the peaks in the spectra of Figure 3.[48] The bathochromic or red shift for the film prepared with PAH solution at pH 4 may be associated with a tilted J-aggregation in the LbL film, according to Advincula et al.[16] For the PAH/PAZO LbL films obtained at pH 4, this may also apply, with the PAZO chromophores adsorbing onto PAH molecules in a tilted orientation, because the PAZO charged group is at the end of the chromophore. This orientation causes the absorption intensity to decrease and the maximum birefringence per chromophore to increase, which explains the higher birefringence ratio attained at pH 4 in the inset of Figure 3.

Analysis of Birefringence Buildup. The buildup of birefringence could be fitted with a two-exponential function, as is usual in the literature,[49−52] with the kinetics comprising two processes:

$$I_{\text{writing}} = I_{w1}\left[1 - \exp\left(-\frac{t}{\tau_{w1}}\right)\right] + I_{w2}\left[1 - \exp\left(-\frac{t}{\tau_{w2}}\right)\right];\ I_{w1} + I_{w2} = 1 \quad (1)$$

where I_{w1} and I_{w2} are pre-exponential factors representing the intensity of the two processes and τ_{w1} and τ_{w2} are the characteristic time constants. The fastest process is normally attributed to the *trans*→*cis*→*trans* photoisomerization dynamics, thus depending on the local mobility of the chromophore in the film. This mobility is dependent on the available free volume and the interaction between the chromophore and the oppositely charged polyelectrolyte, PAH. The second, slower process is related to the mobility of polymer chains, which is dependent on the size of the chain and on interactions with

both polyelectrolytes, manifested as the viscoelastic behavior of the polyelectrolytes.

Figure 4 shows the normalized birefringence signal for the fast (I_{w1}) and slow (I_{w2}) processes. For samples prepared with PAH solution at pH 4, the normalized birefringence for the first, fast process corresponded to 65% of the total birefringence for temperatures up to 60 °C. For 70 °C and above, the first process became less important, with only 35% of the birefringence. Similar trends were observed for the samples prepared at the other pHs, as indicated in Figures 4b and 4c, with the second, slower process dominating at high temperatures. It is worth mentioning that, for pH 6, the fast and slow processes practically give the same contributions at high temperatures.

The characteristic times (τ_{w1} and τ_{w2}) for the birefringence buildup are depicted in Figures 5a and 5b, respectively. The orientation process of the azo-groups, because of photoisomerization, is temperature-dependent, in addition to being dependent on the pH. Upon increasing the temperature, one should expect the characteristic time to decrease, because of the enhanced mobility of the molecules. On the other hand, the number of oriented dipoles tends to decrease due to relaxation. For the films prepared from PAH solutions at pH 4 and pH 6, τ_{w1} decreased as the temperature increased, but it would probably increase again at high temperatures (above T_g, if they were to be reached). Hence, for these samples, the facilitated chromophore movement with increased temperatures overcame the relaxation processes. In contrast, τ_{w1} was minimum at an intermediate temperature (50 °C) for the sample prepared at pH 8, indicating a more balanced competition between the temperature-dependent orienting and relaxation effects. As for the slow process, τ_{w2} was practically temperature-independent for the samples prepared with PAH at pH 4 and pH 6, but increased at high temperatures for the sample obtained at pH 8. The increase in the characteristic time with the temperature for the latter sample suggests the presence of some other type of chromophore orientation, as will be discussed later.

Analysis of Birefringence Relaxation Kinetics. For the sake of comparison, the relaxation curves were normalized with respect to the maximum birefringence for each temperature. The decay curves were also fitted with a two-exponential function, as in Debye processes with two relaxation times:

$$I_{\text{relaxation}} = I_{r1}\exp\left(-\frac{t}{\tau_{r1}}\right) + I_{r2}\exp\left(-\frac{t}{\tau_{r2}}\right);$$
$$I_{r1} + I_{r2} = 1 \qquad (2)$$

where I_{r1} and I_{r2} are the pre-exponential factors for the birefringence normalized intensity taking values between 0 and 1, and τ_{r1} and τ_{r2} are the characteristic time constants of the two processes. As mentioned above, this two-exponential Debye-type behavior is often observed in birefringence decay experiments, in which the fast decay is attributed to dipole disorientation and the slow decay is related to disorientation arising from the movement of polymer chains. Here, the slow process had time constants exceeding tens of hours, so that the overall decay could be represented by an exponential decay for the first process plus a constant I_C that represented the long-term relaxation, as follows:

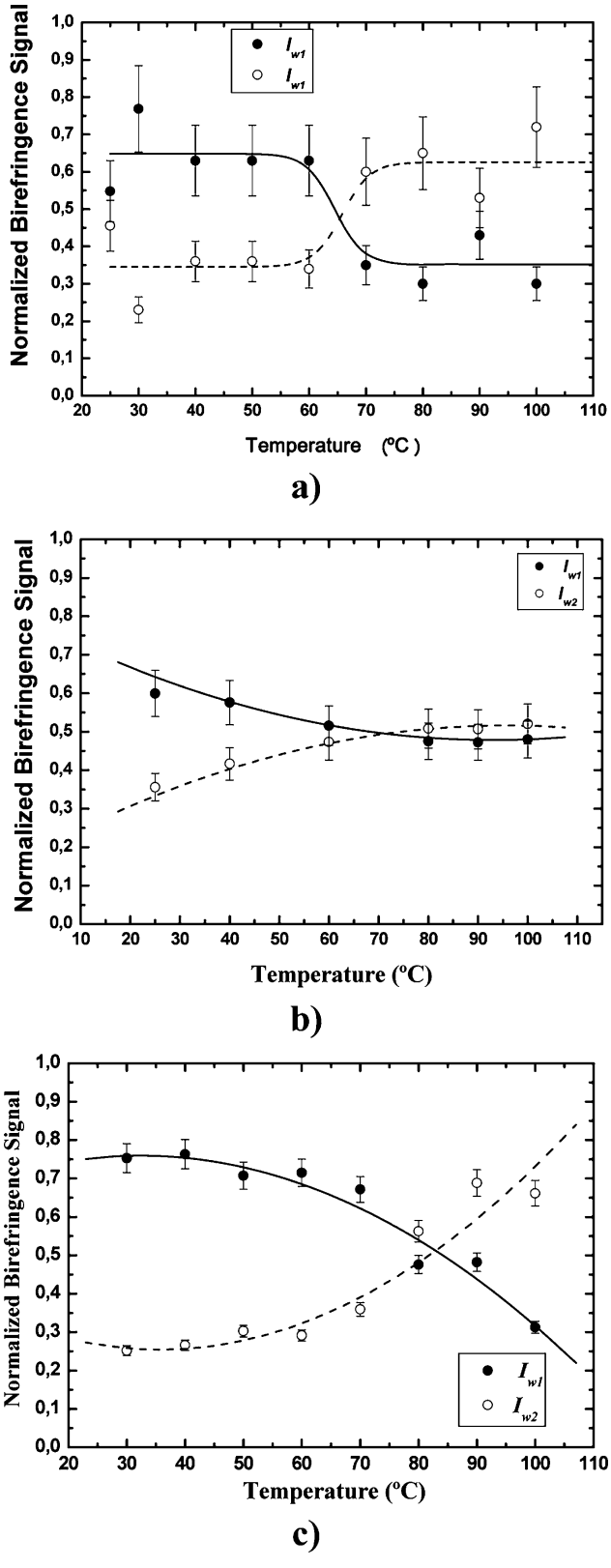

Figure 4. Normalized birefringence intensities, I_{w1} and I_{w2}, as a function of temperature. These parameters were obtained by fitting the buildup data with eq 1 in $(PAH/PAZO)_{20}$ films fabricated from PAH aqueous solutions at (a) pH(PAH) 4, (b) pH(PAH) 6, and (c) pH(PAH) 8. The lines are merely in place to guide the eyes.

dx.doi.org/10.1021/am201722x | ACS Appl. Mater. Interfaces 2012, 4, 1470–1477

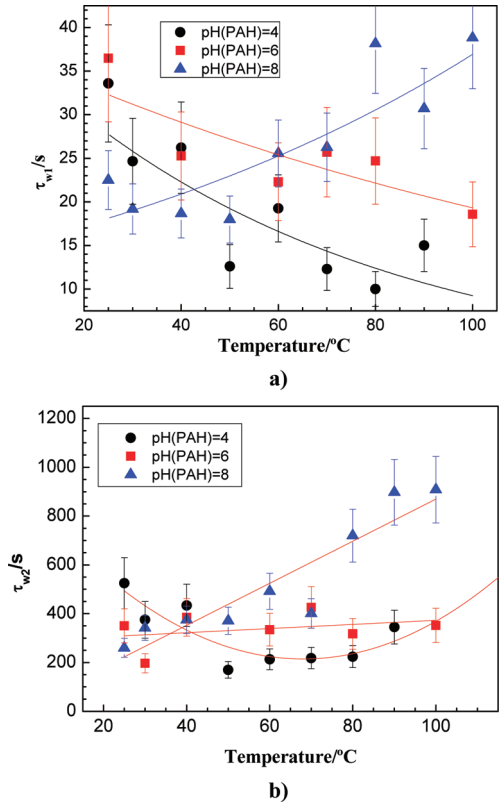

Figure 5. Characteristic times obtained by fitting the buildup data with eq 1 for $(PAH/PAZO)_{20}$ LbL films prepared from pH(PAH) 4, pH(PAH) 6, and pH(PAH) 8: (a) τ_{w1} (fast process) and (b) τ_{w2} (slow process). The lines are only in place to guide the eyes.

$$I_{\text{relaxation}} = I_{r1} \exp\left(-\frac{t}{\tau_{r1}}\right) + I_C; \qquad I_{r1} + I_C = 1 \tag{3}$$

The kinetics for the birefringence after the writing laser was turned off in Figure 2 was fitted using eq 3, with the parameters used being plotted in Figures 6a and 6b. There is little relaxation of the chromophores, with the birefringence being largely preserved. At room temperature, the normalized intensities associated with the fast relaxation process, I_{r1}, correspond to 0.10−0.12 for all three types of samples, i.e., ca. 10% of the total photoinduced birefringence decayed quickly while the remaining 90% decayed with longer characteristic time constants. Here, the birefringence at the end of the experiments is referenced as "residual birefringence". The number of chromophores oriented at higher temperatures is smaller, as indicated in Figure 2b, which is justified by the ease with which dipoles are disoriented at such temperatures. However, the residual birefringence is still high, and the difficulty in disorienting the dipoles can only be explained if the orientation process at high temperatures involves movements of the polymer chains in a way that the chromophores are arranged in more-stable positions. For the film fabricated at pH 8 and near T_g, in particular, there seems to be no relaxation within the time scale of the measurements, as no decrease in birefringence was observed even after 8 h of the argon-ion laser being turned off for a sample kept at 100 °C.

At pH 8, the electrostatic forces between the polyelectrolytes are minimized, because PAH has less charge, but PAZO is ionized. Therefore, the presence of counterions and co-ions,[53]

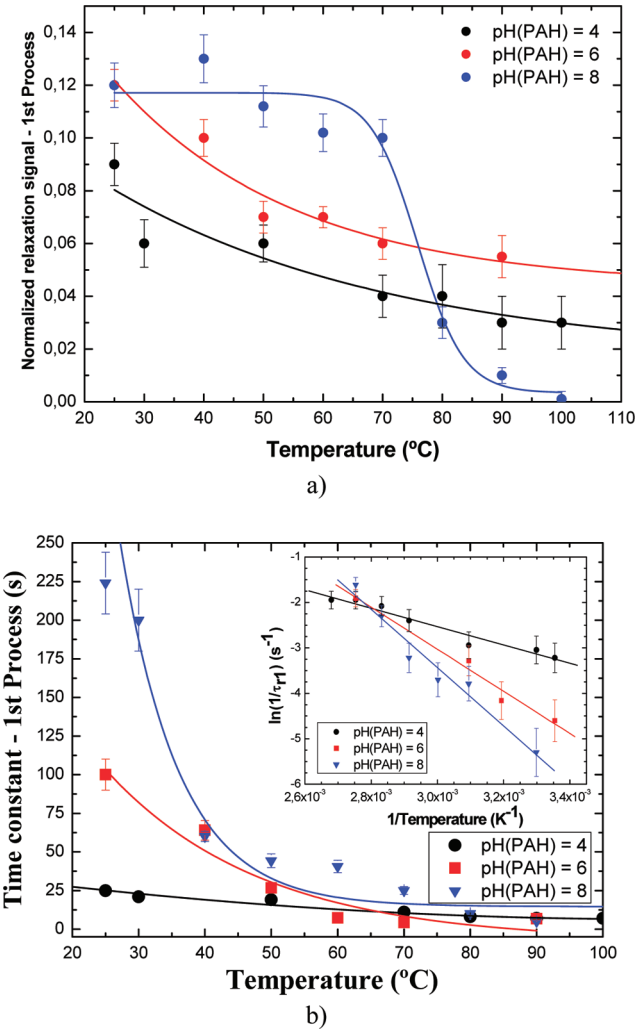

Figure 6. (a) Normalized signal of the first relaxation process (I_{r1}) for PAH/PAZO films made from PAH solutions with different pHs. (b) Characteristic time associated with the first process of the relaxation mechanism for $(PAH/PAZO)_{20}$ LbL films prepared with PAH solutions with different pHs. Arrhenius plots are shown in the inset.

which was inferred from X-ray photoelectron spectroscopy data in PAH/PAZO films,[54] may hinder the orientation of the azo-group.[55] It should also be mentioned that the PAZO molecules are ionized even in films prepared from PAH solutions with pH 4, as demonstrated in the FTIR spectrum (see Figure SI3 in the Supporting Information), where peaks appear in the 1700−1500 cm^{-1} region of the spectrum, assigned to carboxylate (COO−) and carboxylic acid (COOH) groups.[42]

Upon increasing the temperature, the characteristic time constant of the fast process of relaxation decreased, as indicated in Figure 6b), tending to almost the same value for all films. This behavior means that, near the glass transition, the interactions between polyelectrolytes no longer affect the relaxation process. This is consistent with the work of Song et al.,[56] although their explanation was different. They concluded that the fast process was associated with the kinetics of the *cis* isomer while the second, slower process was related to the *trans* isomer. However, this explanation cannot be applied to the results reported here, because the azochromophores would not adopt the *cis* conformation for long.[57]

dx.doi.org/10.1021/am201722x | ACS Appl. Mater. Interfaces 2012, 4, 1470−1477

Table 1. Activation Energies for the Writing and Relaxation Processes in the Buildup and Relaxation Curves, In Addition to the Change in Enthalpy and Entropy Calculated with the Eyring Equation

	Writing Activation Energy (kJ/mol)		Fast Relaxation Process		
pH(PAH)	From τ_{w1}	From τ_{w2}	E_{aR1}(kJ/mol)	ΔH(kJ/mol)	ΔS(kJ K^{-1} mol^{-1})
4	17.4 ± 3.8	18.2 ± 6.3	16.8 ± 1.7	14 ± 2	0.170 ± 0.005
6	6.4 ± 2.0	0.5 ± 1.8	46 ± 14	44 ± 11	0.26 ± 0.04
8	−8.6 ± 2.1	−14.6 ± 2.2	49 ± 4	46 ± 5	0.26 ± 0.02

The residual birefringence is another important parameter, because it reflects the oriented chromophores with long characteristic times. Although this residual birefringence decreased with temperature, as shown in Figure 2a, its normalized value, represented by $I_C = 1 - I_{r1}$ increased until unity for high temperatures. Therefore, chromophores may remain oriented at high temperatures, with the relative number of long-term oriented chromophores even increasing with the temperature. This can only be explained if a temperature-dependent mechanism is used to "freeze" chromophores. Such a mechanism may rely on the presence of counterions near ionic PAZO groups that maintain azochromophores in their *trans* conformation.

Determination of Activation Energies. The results just described lead us to conclude that the temperature affects the competition between the two processes for both the birefringence buildup and relaxation. In order to make this analysis more quantitative, we determined the activation energies for the writing and relaxation processes from Arrhenius plots, using[58]

$$\ln(k_i) = A - \frac{E_a}{R}\left(\frac{1}{T}\right) \tag{4}$$

where k_i is the process rate (s^{-1}) ($k_i = 1/\tau_{wi}$), A a pre-exponential constant, R the universal gas constant ($R = 8.314$ J mol^{-1} K^{-1}), and T the temperature (given in Kelvin). Table 1 gives the activation energies calculated from plotting the logarithm of the reciprocal characteristic times in Figures 5a and 5b, as a function of the inverse of the temperature.

The activation energy for the fast writing process varied from 17.4 kJ/mol for the film fabricated at pH 4 to −8.6 kJ/mol for the film at pH 8. A similar behavior was observed for the activation energy of the second process, with values of 18.2, 0.5, and −14.6 kJ/mol being observed for samples prepared with PAH solutions at pH 4, 6, and 8, respectively. The activation energies of the fast process for samples obtained at pH(PAH) 4 and pH(PAH) 6 are close to those of Langmuir−Blodgett films,[59] particularly for films of 4-[(*N*-ethyl,*N*-2-ethyl-metacryloxy)amino]-2′-chloro-4′-nitroazobenzene and cadmium stearate (HPDR13/CdSt) and of 4-[(*N*-ethyl-*N*-(2-hydroxyethyl)]-amino]-2′-chloro-4′ nitroazobenzene and cadmium stearate (MMA-DR13/CdSt), for which energies of 9.0 ± 0.7 kJ/mol and 14.0 ± 0.9 kJ/mol were obtained, respectively. The much-higher activation energy for the samples at pH 4 is due to PAH being fully charged, with the electrostatic interactions with PAZO groups hindering photoisomerization. The negative activation energy (−8.6 kJ/mol) for the sample prepared at pH(PAH) 8 means that the process cannot be stopped, suggesting that, as the ionic interactions between polyelectrolytes are reduced, the azochromophores are available for orientation without dragging the PAH molecules. Therefore, because a larger number of azo-groups are not bound electrostatically to PAH, the increase in temperature promoted the alignment of azo-chromophores via a cooperative orientation process. Here, we recall that a cooperative interaction in azopolymers upon irradiation has already been demonstrated,[60] where the cooperativity was driven by a few molecules differing in behavior from the majority. In addition, the stability of photoinduced orientation in azopolymers is strongly affected by aggregation.[61]

The energy barrier for relaxation is higher for samples prepared at pH 6 and pH 8, consistent with a more-stable orientation in these films, inferred from the rationale that azochromophores can be oriented cooperatively. We have also used the Eyring equation[62] to investigate the relaxation process, with

$$\frac{1}{\tau} = \frac{k_B T}{\hbar} \exp\left(-\frac{\Delta F}{RT}\right) \tag{5}$$

where τ is the characteristic time constant, k_B the Boltzmann constant, $\hbar$ Planck's constant, R the gas constant, and ΔF the free energy of azo-group relaxation, which can be decomposed in

$$\Delta F = \Delta H - T\Delta S$$

with ΔH being the activation energy for relaxation of the azo-groups and ΔS being the entropy of activation. These parameters were calculated from eq 5 and plotting ln τ_{r1} versus $1/T$. The results in Table 1 indicate that the changes in both enthalpy and entropy related to the fast relaxation process increased with pH. The result for the enthalpy means that it is more difficult to disorient chromophores for samples prepared at higher pHs. As for the entropy results, the larger changes for samples prepared at higher pHs point to more-organized chromophores after the first relaxation process. This is consistent with the cooperative phenomena of aggregation proposed here, and with the increased intensity of the 1260 cm^{-1} band in the FTIR spectrum of the sample subjected to 100 °C (see the Supporting Information).

The importance of the degree of ionization—and, hence, of the electrostatic interactions—was further confirmed by a direct comparison of the pH dependence for the activation energies in the writing processes with that of the degree of ionization. Indeed, Figure 7 shows a similar behavior for the degree of ionization of PAH, as obtained from the data by Choi and Rubner,[43] and the activation energies.

CONCLUSIONS

Photoinduced birefringence was investigated in the temperature range between 25 and 100 °C for poly[1-[4-(3-carboxy-4 hydroxyphenylazo) benzene sulfonamido]-1,2-ethanediyl, sodium salt]/poly(allylamine hydrochloride) (PAZO/PAH) layer-by-layer (LbL) films, in which PAH layers were adsorbed from solutions of different pHs. The dynamics for the birefringence could be described by two processes associated with the orientation of chromophores required for the *trans*−*cis*−*trans* isomerization cycles and with the chain movement. A strong dependence on the PAH solutions pH was observed

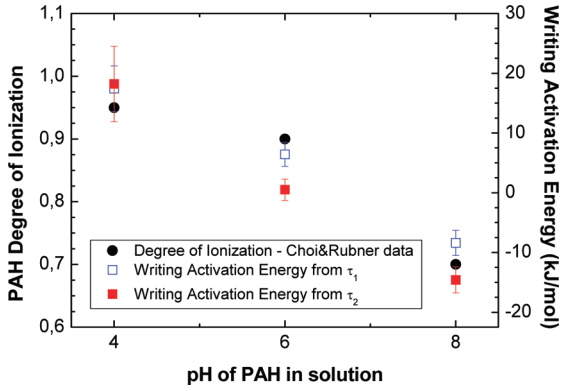

Figure 7. Degree of ionization of PAH in solution obtained from the Choi and Rubner study[43] and the writing activation energies, as a function of the PAH aqueous solution pH.

since, for less-ionized molecules, the *trans* → *cis* → *trans* photoisomerization cycles and chromophores orientation were facilitated. For all films, the maximum birefringence decreased with the temperature, as expected from the literature,[58] because of increased polymer chain flexibility and mobility.

One of the most important features was the higher long-term stability in birefringence at high temperatures for the LbL films produced with low ionized PAH (at high pH). This effect was associated with the presence of co-ions and counterions that may compensate for the electric charge of PAZO chromophores and hinder relaxation. Further evidence for this interpretation came from the activation energies calculated from Arrhenius plots, where a negative energy was obtained for the orientation mechanism for the film prepared at high pH. An important implication of these findings is that the strategy reported here represents an avenue for obtaining long-term stability for birefringence, and at high temperatures, which can be achieved by tuning the electrostatic interactions in LbL films. Applications in stable optical devices, including optical memories, can then be envisaged.

■ ASSOCIATED CONTENT

Supporting Information

This material is available free of charge via the Internet at http://pubs.acs.org.

■ AUTHOR INFORMATION

Corresponding Author

*Tel.: 00351 212948576. E-mail: mfr@fct.unl.pt.

Notes

The authors declare no competing financial interest.

■ ACKNOWLEDGMENTS

This work was supported by the "Plurianual" financial contribution of "Fundação para a Ciência e Tecnologia" (Portugal), through the project POCTI/FAT/47529/2002 (Portugal) and by FAPESP and CNPq (Brazil). This work resulted from taking part in the COST Action CM0601—Electron Controlled Chemical Lithography (ECCL) and in bilateral collaboration projects under the programs CAPES-Brazil/Grices-Portugal and DAAD-Germany/Grices-Portugal.

■ REFERENCES

(1) Decher, G.; Hong, J. D.; Schmitt, J. *Thin Solid Films* **1992**, *210/211*, 831—835.
(2) Decher, G. *Science* **1997**, *277* (5330), 1232—1237.
(3) De Geest, B. G.; Sanders, N. N.; Sukhorukov, G. B.; Demeestera, J.; De Smedt, S. C. *Chem. Soc. Rev.* **2007**, *36*, 636—649.
(4) Li, M.; Ishihara, S.; Akada, M.; Liao, M.; Sang, L.; Hill, J. P.; Krishnan, V.; Ma, Y.; Ariga, K. *J. Am. Chem. Soc.* **2011**, *133*, 7348—7351.
(5) Carrillo, J.-M. Y.; Dobrynin, A. V. *ACS Nano* **2011**, *5* (4), 3010—3019.
(6) Fou, A. C.; Onitsuka, O.; Ferreira, M.; Rubner, M. F.; Hsieh, B. R. *J. Appl. Phys.* **1996**, *79* (10), 7501—7509.
(7) Kotov, N. A; Dekany, I.; Fendler, J. H. *J. Phys. Chem.* **1995**, *99* (35), 13065—13069.
(8) Lee, D. W.; Hong, T.-K.; Kang, D.; Lee, J.; Heo, M.; Kim, J. Y.; Kim, B.-S.; Shin, H. S. *J. Mater. Chem.* **2011**, *21*, 3438—3442.
(9) Chen, Q.; Worfolk, B. J.; Hauger, T. C.; Al-Atar, U.; Harris, K. D.; Buriak, J. M. *ACS Appl. Mater. Interfaces* **2011**, *3* (10), 3962—3970.
(10) Balasubramanian, S; Wang, X. G.; Wang, H. C.; Yang, K.; Kumar, J.; Tripathy, S. K.; Li, L. *Chem. Mater.* **1998**, *10* (6), 1554—1560.
(11) Dante, S.; Advincula, R.; Frank, C. W.; Stroeve, P. *Langmuir* **1999**, *15*, 193—201.
(12) Lee, S.H .; Balasubramanian, S.; Kim, D. Y.; Viswanathan, N. K.; Bian, S.; Kumar, J.; Tripathy, S. K. *Macromolecules* **2000**, *33* (17), 6534—6540.
(13) Kaneko, F.; Kato, T.; Baba, A; Shinbo, K.; Kato, K; Advincula, R. C. *Colloids Surf. A* **2002**, *198—200*, 805—810.
(14) Patton, D; Park, M.-K.; Wang, S.; Advincula, R. C. *Langmuir* **2002**, *18*, 1688—169.
(15) Park, M.-K.; Advincula, R. C. *Langmuir* **2002**, *18*, 4532—453.
(16) Advincula, R. C.; Fells, E.; Park, M.-K. *Chem. Mater.* **2001**, *13* (9), 2870—2878.
(17) Ahmad, N. M.; Saqib, M.; Barrett, C. J. *J. Macromol. Sci., Part A: Pure Appl. Chem.* **2010**, *47*, 534—544.
(18) Oliveira, O. N., Jr.; He, J.-A.; Zucolotto, V.; Balasubramanian, S.; Li, L.; Nalwa, H. S.; Kumar, J.; Tripathy, S. K. Layer-by-Layer Polyelectrolyte-Based Thin Films for Electronic and Photonic Applications. In *Handbook of Polyelectrolytes and Their Applications*; Tripathy, S. K., Kumar, J., Nalwa, H. S., Eds; American Scientific Publishers: Stevenson Ranch, CA, 2002, Vol. *1*, p 1.
(19) Barrett, C.; Natansohn, A.; Rochon, P. *Macromolecules* **1994**, *27*, 4781—4786.
(20) Barrett, C.; Natansohn, A.; Rochon, P. *Chem. Mater.* **1995**, *7*, 899—903.
(21) Meng, X.; Natansohn, A.; Barrett, C.; Rochon, P. *Macromolecules* **1996**, *29*, 946—952.
(22) Tanchak, O. M.; Barrett, C. J. *Macromolecules* **2005**, *38* (25), 10566—10570.
(23) Mysliwiec, J.; Miniewicz, A.; Nespurek, S.; Studenovsky, M.; Sedlakova, Z. *Opt. Mater.* **2007**, *29*, 1756—1762.
(24) Shinbo, K.; Baba, A.; Kaneko, F.; Kato, T.; Kato, K.; Advincula, R. C.; Knoll, W. *Mater. Sci. Eng., C* **2002**, *22*, 319—325.
(25) Jiang, X. L.; Li, L.; Kumar, J.; Kim, D. Y.; Tripathy, S. K. *Appl. Phys. Lett.* **1998**, *72*, 2502—2504.
(26) Xue, X.; Zhu, J.; Zhan, Z.; Zhou, N.; Zhu, X. *React. Funct. Polym.* **2010**, *70*, 456—462.
(27) Pan, Y.; Tang, X. *Synth. Met.* **2009**, *159*, 1796—1799.
(28) Jiang, X.; Chen, X.; Yue, X.; Zhang, J.; Chen, Q. *React. Funct. Polym.* **2010**, *70*, 616—621.
(29) Nicolescu, F. A.; Jerca, V. V.; Vuluga, D. M.; Vasilescu, D. S. *Polym. Bull.* **2010**, *65*, 905—916.
(30) Xu, X.; Zhou, N.; Zhu, J.; Tu, Y.; Zhang, Z.; Cheng, Z.; Zhu, X. *Macromol. Rapid Commun.* **2010**, *31*, 1791—1797.
(31) Kulikovsky, L.; Kulikovska, O.; Goldenberg, L. M.; Stumpe, J. *ACS Appl. Mater. Interfaces* **2009**, *1* (8), 1739—1746.
(32) Wang, H. P.; He, Y. N.; Tuo, X. L.; Wang, X. G. *Acta Polym. Sin.* **2003**, *5*, 620—625.
(33) Torodov, T.; Nikolova, L.; Tomova, N. *Appl. Opt.* **1984**, *23*, 4309—4312.

(34) Rochon, P.; Gosselin, J.; Natansohn, A.; Xie, S. *Appl. Phys. Lett.* **1992**, *60*, 4−5.
(35) Natansohn, A.; Rochon, P.; Gosselin, J.; Xie, S. *Macromolecules* **1992**, *25*, 2268−2273.
(36) Song, O. K.; Wang, C. H.; Pauley, M. A. *Macromolecules* **1997**, *30*, 6913−6919.
(37) Delaire, J. A.; Nakatani, K. *Chem. Rev.* **2000**, *100*, 1817−1845.
(38) Mateev, V.; Markovsky, P.; Nikolova, L.; Todorov, T. *J. Phys. Chem.* **1992**, *96*, 3055−3058.
(39) Meng, X.; Natanshon, A.; Rochon, P. *J. Polym. Sci., Part B: Polym. Phys.* **1996**, *34*, 1461−1466.
(40) Xu, G.; Si, J.; Liu, X.; Yang, Q. G.; Ye, P.; Li, Z.; Shen, Y. *J. Appl. Phys.* **1999**, *85* (2), 681−685.
(41) Dall'Agnoll, F. F.; Souza, N. C.; de; Oliveira, O. N. Jr.; Giacometti, J. A. *Synth. Met.* **2003**, *138*, 153−156.
(42) Ferreira, Q.; Gomes, P. J.; Raposo, M.; Giacometti, J. A.; Oliveira, O. N. Jr.; Ribeiro, P. A. *J. Nanosci. Nanotechnol.* **2007**, *7*, 2659−2666.
(43) Choi, J.; Rubner, M. F. *Macromolecules* **2005**, *38*, 116−124.
(44) Itano, K.; Choi, J.; Rubner, M. F. *Macromolecules* **2005**, *38*, 3450−3460.
(45) Hiller, J.; Rubner, M. F. *Macromolecules* **2003**, *36*, 4078−4083.
(46) Ferreira, Q.; Gomes, P. J.; Maneira, M. J. P.; Ribeiro, P. A.; Raposo, M. *Sens. Actuators, B* **2007**, *126*, 311−317.
(47) Taniike, K.; Matsumoto, T.; Sato, T.; Ozaki, Y.; Nakashima, K.; Iriyama, K. *J. Phys. Chem.* **1996**, *100* (38), 15508−15516.
(48) Ariga, K.; Lvov, Y; Kunitake, T. *J. Am. Chem. Soc.* **1997**, *119*, 2224−2231.
(49) Xu, G.; Jinhai, S.; Liu, X.; Yang, Q. G.; Ye, P.; Li, Z.; Shen., Y. *J. Appl. Phys.* **1999**, *85*, 681−685.
(50) Wu, Y.; Kanazawa, A.; Shiono, T.; Ikeda, T.; Zhang, Q. *Polymer* **1999**, *40*, 4787−4793.
(51) Natansohn, A.; Rochon, P. *Chem. Rev.* **2002**, *102*, 4139−4175.
(52) Ho, M. S.; Natansohn, A.; Rochon, P. *Macromolecules* **1995**, *28*, 6124−6127.
(53) Lourenço, J. M. C.; Ribeiro, P. A; Botelho do Rego, A. M.; Braz Fernandes, F. M.; Moutinho, A. M. C.; Raposo, M. *Langmuir* **2004**, *20*, 8103−8109.
(54) Ferreira, Q. Ph.D. Thesis, Faculty of Science and Technology of the New University of Lisbon (FCT/UNL), Caparica, Portugal, 2007, p 110.
(55) Madruga, C.; Alliprandini Filho, P.; Andrade, M. M.; Gonçalves, M.; Raposo, M.; Ribeiro, P. A. *Thin Solid Films* **2011**, *519*, 8191−8196.
(56) Song, O.-K.; Wang, C. H.; Pauley, M. A. *Macromolecules* **1997**, *30*, 6913−6919.
(57) Natansohn, A.; Rochon, P. *Macromolecules* **1998**, *31*, 7960−7961.
(58) Freiberg, S.; Lagugné-Labarthet, F.; Rochon, P.; Natanshon, A. *Can. J. Chem.* **2004**, *82*, 1−10.
(59) Dall'Agnoll, F. F.; de Souza, N. C.; Oliveira, O. N. Jr.; Giacometti, J. A. *Synt. Met.* **2003**, *138*, 153−156.
(60) Barille, R.; Ahmadi-Kandjani, S.; Ortyl, E.; Kucharski, S.; Nunzi, J.-M. *New J. Chem.* **2009**, *33*, 1207−1210.
(61) Lagugné-Labarthet, F.; Freiberg, S.; Pellerin, C.; Pézolet, M.; Natansohn, A.; Rochon, P. *Macromolecules* **2000**, *33*, 6815−6823.
(62) Eyring, H. *J. Chem. Phys.* **1936**, *4*, 283−291.